

# AN ASSESSMENT OF ONE-DIMENSIONAL APPROACH FOR STRUCTURAL MODELING OF COMPOSITE HELICOPTER ROTOR BLADES FOR AEROELASTIC ANALYSIS

Murat Sahin,  
mursahin@tai.com.tr, TAI-Turkish Aerospace Industries Inc., Ankara, Turkey  
Evren Taskinoglu,  
etaskinoglu@tai.com.tr, TAI-Turkish Aerospace Industries Inc., Ankara, Turkey  
Gokhan Tursun,  
gtursun@tai.com.tr, TAI-Turkish Aerospace Industries Inc., Ankara, Turkey  
Serdar Dilaver,  
sdilaver@tai.com.tr, TAI-Turkish Aerospace Industries Inc., Ankara, Turkey

## Abstract

Helicopter rotor blade models are required to address different analysis requirements with demanding modelling challenges and yet are expected to provide high accuracy with low-calculation cost. This study aims to present an assessment of modeling accuracy of a nonlinear beam approach for composite helicopter rotor blades. Static deflection, free-vibration and transient forced response analyses are conducted for the study. Nonlinear beam analysis results are compared with MSC.NASTRAN FE results and experimental measurements from published studies; parameters effective on modeling accuracy are underlined.

## 1. INTRODUCTION

Helicopter rotor blade design is a challenging work which requires a multidisciplinary approach and an iterative process. An optimized solution for performance, vibration and noise is expected with constraints for aeroelastic stability, structural integrity and manufacturing. Consistently, analysis models are required to provide low calculation cost and high accuracy at the same time. Beam approaches are good candidates for modeling of helicopter rotor blades due to the slender nature of the blade structure and still today, find extensive use particularly for aeroelastic analyses due to the incomparable computational efficiency benefit and convenience in integration with other tools. However current rotor blade designs require more developed theories for an adequate representation of the blade structure.

Motivation for this study comes from the need to provide an assessment for modeling accuracy of a nonlinear beam approach for composite helicopter rotor blades. The beam model is expected to address aeroelastic response, aeroelastic stability and vibration analysis requirements for different rotor design configurations of today and moreover meet the demanding modeling challenges of the composite twisted blade structure. The study presented here benefits from the results of validation

studies in the literature and adds to the previous research work on assessment of structural models [1] [2] [3] for helicopter rotor blades.

In this work, a Timoshenko-like geometrically exact nonlinear beam model based on the formulation of mixed variational exact intrinsic equations approach [4] is studied which can model geometric nonlinearities, warping deformations and elastic couplings of curved and twisted beam structures. This formulation, together with an analysis method for cross-sectional properties, provides unified nonlinear analysis for non-homogenous, anisotropic beams as proposed in the work [5] of Atilgan and Hodges. The approach basically studies the geometrically nonlinear 3D beam problem separately as a nonlinear-one dimensional problem and a linear two-dimensional problem. The two-dimensional problem or in other words, sectional analysis for extraction of elastic constants is a crucial part of beam modeling study. Stiffness constants are input to the 1D beam formulation and hence determination of these properties is an independent problem in terms of accuracy. In this work, sectional analysis results will be reviewed for the assessment of the beam modeling accuracy and VABS II cross-sectional analysis is conducted for several cases.

The model used in this study for one-dimensional solution is based on the finite-element implementation of the mentioned nonlinear beam theory which is referred to as mixed variational

formulation based on exact intrinsic equations of motion for dynamics of moving beams as published in the work [6] of Shang. Soykasap [7] continued the work using the mixed variational formulation to conduct a study for aeroelastic optimization of a composite tilt-rotor and later Cheng [8] extended the work into time-domain using finite-difference discretization and time integration.

## 2. METHOD

In this study, assessment of the beam modeling accuracy will be based on a correlation effort of the nonlinear beam analysis results with MSC.NASTRAN FE results and experimental measurements mainly from published studies. Static deflection, free-vibration and transient forced response analyses are conducted for the study. In this work, three cases are investigated: thin strip laminated beams of Minguet [9], elastically coupled closed box beam of Chandra [10] and a hypothetical main rotor blade with constant cross-section.

## 3. ANALYSIS MODELS

The analysis models used in the study are described in below. The models are the mixed variational formulation nonlinear beam analysis model and MSC.NASTRAN FE code.

### 3.1 Mixed Variational Formulation – Nonlinear Geometrically Exact Beam Model

The model used in this study is based on the finite-element implementation of mixed variational formulation based on exact intrinsic equations of motion for dynamics of moving beams as published in the work [6] of Shang. The model will be referred in this text hereafter with the title “MVF analysis model”. The formulation provides nonlinear geometrically exact analysis of one-dimensional beam. Below provided is a brief summary of formulation and finite element discretization as defined in Shang’s work; the reader can refer to this reference and the original work of Hodges [4] for more details.

Reference frames for application of the mixed variational formulation are: the rotating global frame  $a$ , the beam undeformed reference frame  $b$  and beam deformed frame  $B$ ; an illustration is provided below in Figure 1. Subscripts  $a$ ,  $b$  and  $B$  in the following notation denote the defined frame for the quantities. In Shang’s [6] application of mixed variational formulation for dynamics of moving beams [4] displacement and rotational variables are

measured in the global reference frame  $a$ ; however force, strain, velocity and momentum are measured in deformed beam frame  $B$ .

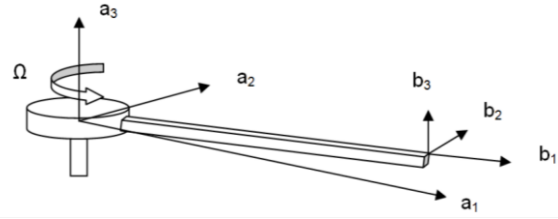


**Figure 1. Global reference frame ‘a’ and undeformed reference frame ‘b’ [1]**

Mixed variational formulation is derived from the extended form of Hamilton’s principle as follows:

$$(1) \int_{t_1}^{t_2} \int_0^l [\delta(K - U) + \delta\bar{W}] dr dt = \delta\bar{A}$$

where  $K$  and  $U$  are the kinetic and strain energy densities per unit length respectively,  $\delta\bar{A}$  is the virtual action at the ends of the time interval:  $t_1$  and  $t_2$ , and  $\delta\bar{W}$  is the virtual work of the applied loading per unit length.

Internal force and moment vectors  $F_B$  and  $M_B$  are defined as variation of strain energy term with respect to general strain vectors  $\gamma$  and  $\kappa$ ; whereas the linear and angular momentum vectors  $P_B$  and  $H_B$  are defined as variation of kinetic energy term with respect to linear and angular velocities  $V_B$  and  $\Omega_B$ .

$$(2) F_B = \left( \frac{\partial U}{\partial \gamma} \right)^T \quad M_B = \left( \frac{\partial U}{\partial \kappa} \right)^T \quad P_B = \left( \frac{\partial K}{\partial V_B} \right)^T \quad H_B = \left( \frac{\partial K}{\partial \Omega_B} \right)^T$$

The equation of motion can be written as below:

$$(3) \int_{t_1}^{t_2} \int_0^l [\delta V_B^{*T} P_B + \delta \Omega_B^{*T} H_B - \delta \gamma^{*T} F_B - \delta \kappa^{*T} M_B] + \int_{t_1}^{t_2} \int_0^l \delta \bar{W} dt = \delta \bar{A}$$

Geometrically exact equations for strain and velocity are as follows:

$$(4) \gamma^* = C^{Ba} (C^{ab} e_1 + u_a') - e_1 \quad \kappa^* = C^{ba} \left( \frac{\Delta - \tilde{\theta}}{1 + \frac{\theta^T \theta}{4}} \right) \theta'$$

$$(5) V_B^* = C^{Ba} (v_a + \dot{u}_a + \tilde{\omega}_a u_a) \quad \Omega_B^* = C^{ba} \left( \frac{\Delta - \tilde{\theta}}{1 + \frac{\theta^T \theta}{4}} \right) \dot{\theta} + C^{Ba} \omega_a$$

where  $C^{Ba}$ ,  $C^{ab}$  and  $C^{ba}$  are the transformation matrices,  $u_a$  is the displacement vector,  $\Delta$  is the 3x3 identity matrix,  $\theta$  is the rotation vector and  $\tilde{\theta}$  is the dual matrix representation of the rotation matrix,  $u_a$  is the initial translational velocity and  $\omega_a$  is the initial angular velocity.

Constitutive relations between force/moment and strain and between momentum and velocity quantities are defined as follows:

$$(6) \quad \begin{Bmatrix} F_B \\ M_B \end{Bmatrix} = [S] \begin{Bmatrix} \gamma \\ \kappa \end{Bmatrix}, \quad \begin{Bmatrix} P_B \\ H_B \end{Bmatrix} = \begin{bmatrix} m\Delta & -m_e \\ m_e & I \end{bmatrix} \begin{Bmatrix} V_B \\ \Omega_B \end{Bmatrix}$$

where  $m$  is mass per unit length,  $m_e$  is the offset between beam reference line and mass center,  $I$  is the moment of inertia and  $S$  is 6x6 stiffness matrix.

Finite element discretization is performed in spatial domain with the equation of motion in the following form:

$$(7) \quad \int_{t_1}^{t_2} \sum_i \delta \Pi_i dt = 0$$

For time integration, second-order backward Euler method discretization in Cheng's work [8] is adopted.

### 3.2 MSC.NASTRAN FEM

Analysis results of commercial general-purpose finite element MSC.NASTRAN are compared with the nonlinear beam model for all cases. PCOMP entry is used with QUAD4 shell elements to model the composite laminated beams and SOL 106 nonlinear solver is chosen. "nlgyroa.alt" DMAP alter modification is used with SOL 106 nonlinear solution sequence for rotational effects. Forced response analysis is conducted with SOL 112 modal transient response solution.

## 4. RESULTS AND DISCUSSIONS

### 4.1 Case A - Thin Strip Laminated Beam

For this case, thin strip laminated beams in the experimental work of Minguet [9] [11] are studied. In the referenced works, static bending tests and experimental identification of natural frequencies were conducted for composite laminated beams with different layups.

The beams have rectangular cross-section with a width of 30 mm and length of the beam is noted as

550 mm for static deflection specimens and 560 mm for natural frequency analysis. Ply material is AS4/3501-6 graphite/epoxy and ply properties are  $E_1=142$  GPa,  $E_2=9.8$  GPa,  $G_{12}=6$  GPa,  $\nu_{12}=0.3$ ,  $t_{ply}=0.134$  mm and  $\rho=1580$  kg/m<sup>3</sup>. Two different laminates are investigated in this study:  $[45/0]_{3s}$  and antisymmetric layup of  $[20/-70/-70/20]_{2a}$ .  $[45/0]_{3s}$  layup exhibits bending-twist and  $[20/-70/-70/20]_{2a}$  is expected to show extension-twist coupling.

The modeling of the beam is realized with only 11 elements for MVF analysis. MSC.NASTRAN uses composite shell properties with 220 QUAD4 elements and follows SOL 106 nonlinear solution sequence for static analysis and prestressed normal modes analysis. MVF analysis is based on the laminate properties presented in the reference [9] which provides 6x6 stiffness matrix inputs and VABS II results. It should be noted that the thickness of the laminate is an important modeling parameter. In the work of Minguet [9] it was reported that sectional properties were based on the laminate thickness measured after the nonstructural epoxy layer was removed following the curing operation. In this study, "effective laminate thickness" suggestion of Minguet [9] is followed and therefore MSC.NASTRAN shell models are constructed with ply thicknesses modified according to laminate thickness measured after extra coated resin is removed. "Effective ply thickness" shows better correlation as is shown in referenced works [1] [12].

Beam analysis is directly dependent on the stiffness constants; sectional analysis results are presented in tables 1, 2 and 3 for  $[0/90]_{3s}$ ,  $[45/0]_{3s}$  and  $[20/-70/-70/20]_{2a}$  laminates. Note that VABS II analysis results are close to NABSA [12] and VABS [12] results in the references, however is considerably different from results in the work of Minguet [9].

#### 4.1.1. Static Analysis for Case A

Static deflection results are provided in Figures 2 and 3 for NASTRAN solution, MVF beam analysis with Minguet [9] sectional properties and MVF beam analysis with VABS II sectional properties. For the layup  $[45/0]_{3s}$ , MVF analysis, NASTRAN model and experimental measurements are all in very good agreement for vertical and horizontal deformations; however axial deformation measurement shows discrepancy. For  $[20/-70/-70/20]_{2a}$  layup, MVF analysis with Minguet [9] sectional properties predicts less deformation for vertical and axial displacement; for this case MSC.NASTRAN model and beam analysis with VABS II sectional properties are observed to be in better agreement with experimental results. It should be noted that 1D nonlinear beam deformation results are only as accurate as the sectional properties used in the

modeling and more investigation should be done with different elastic constants.

#### 4.1.2. Free Vibration Analysis for Case A

In the referenced work [11], an experimental identification study of natural frequencies of the thin strip cantilevered beams are provided. Results for  $[0/90]_{3s}$ ,  $[45/0]_{3s}$  and  $[20/-70/-70/20]_{2a}$  laminates are shown in Table 4. Analysis results are close to experimental measurements in general; the discrepancy is larger for 3<sup>rd</sup> flap mode and torsion. Laminate properties used for beam analysis results are those, provided in the reference study [9] and VABS II results. Composite shell modeling is based on effective ply thickness which shows good correlation in static deflection results. Better results using MVF analysis are obtained by increasing the number of elements in higher modes. Analysis results are reported for both the density according to ply properties and the density normalized according to laminate thickness; however one cannot conclude that any of the two density choices shows better correlation with experimental readings for all layup results.

In addition to elastic constants, inertia matrix has naturally strong influence on the results; however since constructing the inertia matrix does not require a dedicated analysis procedure, it has not taken a particular attention in literature. Translational inertia matrix (mass matrix  $[m_1, m_2, m_3]$ ) has direct influence on bending modes, note that however torsional frequency is strongly sensitive to the I11 rotational inertia term. Rotational inertia terms, in opposite, do not create a significant delta on bending modes for the laminated beams investigated.

For  $[45/0]_{3s}$  laminate, note that NABSA and VABS predictions from the ref.12 have a different S12 stiffness value other than VABS II. However this difference has almost no influence on the presented natural frequencies. The same is also true for the S33 prediction. VABS [12] results show a considerably different S33 stiffness value other than NABSA and VABS II as well; which has again only a very little influence over flap modes.

According to NASTRAN results,  $[45/0]_{3s}$  laminate shows a slight coupling for flap modes for both prestressed and stress-free solutions; this can be attributed to the bending-twist coupling. The same effect can also be observed in beam analysis results. Beam analysis also shows, in response, a slight coupling of the torsional mode with third flap mode; however this cannot be observed from NASTRAN analysis results.

For  $[20/-70/-70/20]_{2a}$  laminate, the major discrepancy between NABSA, VABS [12] and VABS II stiffness predictions are for S33 term which is almost an order (10 times) difference between these code outputs. However, S33 term is shown to have no noticeable effect.

In Ref.13 the same bending-twist and extension-twist coupled beams of Minguet were studied; similarly the authors pointed out the insensitivity of natural frequencies with respect to large differences in shear rigidities as in here, however they argued that this difference may be more important for higher modes.

#### 4.2. Case B - Elastically Coupled Closed Box Beam

In this case, a thin-walled rectangular cross-section box beam specimen from Chandra [10] is studied. The beam has the circumferentially asymmetric stiffness (CAS) layup (also denoted as symmetric configuration) of  $[45]_6$  which produces bending-twist coupling. The material is AS4/3501-6 graphite epoxy as in Case A, with Poisson's ratio is now reported as  $\nu_{12}=0.42$  [10]. Inner dimension of the rectangular cross section is  $0.893 \times 0.477$  in. and length of the beam is 33.25 in. Ply thickness is 0.005 in. resulting in 0.030 in. wall thickness for 6 plies and mass density is  $0.1352 \times 10^{-3}$  lb s<sup>2</sup>/in.

For the rotating beam, MVF analysis is performed with 20 elements and NASTRAN model includes 900 CQUAD4 elements. Both 4x4 stiffness results from Cesnik's work [12] and 6x6 VABS II analysis results are used as input for MVF analysis.

##### 4.2.1. Free Vibration Analysis for Case B

Chandra and Chopra [14] conducted a study in an in-vacuo rotor test facility to experimentally obtain rotating natural frequency of the same layup at different rotational speeds.

The results are provided in Figure 4 for 1<sup>st</sup> and 2<sup>nd</sup> flap (out-of-plane) and 1<sup>st</sup> lag (in-plane) modes. NASTRAN modeling and MVF analysis results both according to sectional analysis of Ref.12 and VABS II stiffness constants are in very good agreement with variation not exceeding 2.5%. Correlation with experimental data is found unsatisfactory for 2<sup>nd</sup> flap mode for which, stiffening with increasing frequency follows a different trend; however for 1<sup>st</sup> flap and lag modes, correlation is satisfactory.

#### 4.2.2. Transient Forced Response Analysis for Case B

In this part of the study, the transient forced time response results of MSC.NASTRAN FE code and MVF analysis are compared for the same composite thin-walled box beam for a harmonic loading in time domain. The analysis is carried on at a constant rotating speed of 80 rad/s. The forcing is applied for 1 second vertically at the free tip of the cantilever beam and is of 1 N magnitude; vertical tip displacement results are plotted in Figures 5 and 6 for 10 Hz and 80 Hz sinusoidal forcing signals. For the analysis, MSC.NASTRAN SOL 112 modal transient time response solution sequence with 20 modes for eigenvalue extraction is chosen. Solution time step is set 0.001 s for both analysis methods.

Beam analysis is conducted with only 4x4 VABS [12] results. For rotation at 80 rad/s, natural frequencies are as follows: MVF solution results in 20.40 and 99.20 Hz for the first two flap modes and NASTRAN results are recorded as 20.09 and 97.00 Hz. For the forcing frequency of 10 Hz, it is expected that the first flapping mode is excited dominantly; whereas for 80 Hz excitation a multi-frequency response is anticipated. According to the recorded natural frequencies from free-vibration analysis, MVF and NASTRAN models are expected to bear very similar results. In accordance with this expectation, for 10 Hz excitation, presented forced response plots are almost identical for MVF and NASTRAN analysis.

For 80 Hz excitation, a correlation is more difficult since more frequency components exist and at higher frequencies beam results are expected to deviate from the original 3 dimensional problem. Even though the natural frequencies are very close, mode shapes may exhibit a slightly different behavior which would eventually result in a different transient response time history. Note that VABS uses the small parameter  $h/L$  (along with others) for dimensional reduction from the original problem, where  $h$  is characteristic cross-sectional dimension and  $L$  is the characteristic wavelength of deformation. Characteristic wavelength  $L$  decreases with higher modes and as would be expected, accuracy decreases as well.

#### 4.3. Case C- Hypothetical Main Rotor Blade

For this case, a hypothetical main rotor blade with composite construction which has constant cross-section profile/properties is studied. The design does not include twist, curvature, droop or elastic couplings for simplification. In this example, it is intended to investigate the modeling accuracy of the beam approach for a realistic blade cross-section with different materials.

The material for all plies is AS4/3501-6 graphite epoxy as in Case A. The hypothetical design has a simple c-shaped laminated spar with 8 zero degree plies. Skin structure is a 4 ply-laminate with [45/-45]<sub>s</sub> layup and wraps around the whole airfoil profile as a single laminate. Blade has a rohocell core starting at around 30% of the chord at exactly where the spar structure ends; the isotropic rohocell core material has properties:  $E=100$  MPa,  $\nu=0.33$  and  $\rho=75$  kg/m<sup>3</sup>. Rohacell core, despite its small contribution to stiffness in a sectional analysis for beam, has influence on mode shapes and hence possibly frequencies for the FE model.

The film adhesive at the trailing edge is significant since it has a major contribution to torsional stiffness. Adhesive is modeled as isotropic material with  $E=1000$  MPa,  $\nu=0.33$  and  $\rho=1000$  kg/m<sup>3</sup>.

The blade is modeled with cantilever boundary condition which is representative of a bearingless rotor or a teetering/gimballed rotor in hover. NACA0012 airfoil is chosen. Rotor radius is 2 meters, chord length 0.16 m and rotor nominal speed is 10 hz.

For this case, a FE model in NASTRAN and MVF beam model are constructed. NASTRAN FE model uses shell properties for skin and spar laminated structure; laminate properties are created in MSC. Laminate Modeler. Rohacell Core and trailing-edge film adhesive are modeled using solid elements. 11800 HEX8 solid elements and 18000 QUAD4 elements are used in the modeling. For beam modeling, sectional properties are created in VABS II. Mesh is constructed with 1884 4-noded elements. Beam model is realized with 10 and 20 elements.

#### 4.3.1. Free vibration analysis for Case C

Natural frequency analysis results are presented in Figure 7; MVF analysis NASTRAN FE model results are included. Correlation is considered to be very successful for the first flap, first lag and second flap modes with error rate increasing for higher modes as expected.

Note that sectional analysis with VABS II is studied with different mesh refinement; for the selected discretization level (1884 elements), the sectional analysis solution for elastic constants is thought to be converged since variation in beam analysis results does not show noticeable difference. Similarly 20 elements are shown to be accurate enough; the result for 10 element solution is not plotted, because it is almost identical.

## 5. CONCLUSIONS

In this work, a comparison study was conducted to make an assessment of one-dimensional structural modeling approach for composite helicopter rotor blades. Several cases are investigated, each to test and compare a different aspect of modeling and in analysis of cases also a bottom-up approach is adopted. Analysis studies include: elastically coupled thin strip laminated and closed box beams and a hypothetical main rotor blade. For the study, a nonlinear geometrically exact beam model analysis results for static deflection, free vibration, transient forced time response are evaluated with MSC.NASTRAN FE code results and experimental measurements reported in references where available. Correlation with experimental readings and MSC.NASTRAN FEM is shown to be in good agreement for the studied cases.

## 6. ACKNOWLEDGMENTS

This research is partly a product of the effort carried out for a TEYDEB project supported by TUBITAK (The Scientific and Technological Research Council of Turkey). The support is sincerely appreciated.

The first author would like to express thanks to Prof.Dr.Ömer Soykasap from Afyon Kocatepe University for his valuable support in the project and his help in understanding nonlinear composite beam theory.

## 7. REFERENCES

- [1] Sahin, M., Soykasap, O. and Satioglu, Y.C., Comparison Study on Rigorous Structural Modeling of Composite Rotor Blades, 52nd AIAA/ASME/ASCE/AHS/ASC Structures, Structural Dynamics, and Materials Conference, Denver, Colorado, 4-7 April 2011.
- [2] Yeo, H., Truong, K. V., and Ormiston, R. A., Assessment of 1-D Versus 3-D Methods for Modeling Rotor Blade Structural Dynamics, 51st AIAA/ASME/ASCE/AHS/ASC Structures, Structural Dynamics, and Materials Conference, Orlando, Florida, 12 - 15 April 2010.
- [3] Volovoi, V. V., Hodges, D. H., Cesnik, C. E. S., and Popescu B., Assessment of Beam Modeling Methods for Rotor Blade Applications Mathematical and Computer Modelling, Vol. 33, p. 1099-1112., 2001.
- [4] Hodges, D. H., A Mixed Variational Formulation Based on Exact Intrinsic Equations for Dynamics of Moving Beams, Journal of Solids and Structures, Vol. 26, p. 1253-1273., 1990.
- [5] Atilgan, A. R., and Hodges, D. H., Unified Nonlinear Analysis for Nonhomogenous Anisotropic Beams with Closed Cross Sections, AIAA Journal, Vol.29, No. 11, p. 1990-1999., 1991.
- [6] Shang, X., Aeroelastic Stability of Composite Hingeless Rotors with Finite-State Unsteady Aerodynamics, Ph.D. Dissertation, School of Aerospace Engineering, Georgia Institute of Technology, Atlanta, GA, 1995.
- [7] Soykasap, O., Performance Enhancement of a Composite Tilt-Rotor Using Aeroelastic Tailoring, Journal of Aircraft, Vol. 37, No. 5, 2000, pp. 850-858.
- [8] Cheng, T., Structural Dynamics Modeling of Helicopter Blades for Computational Aeroelasticity, M.Sc.Thesis, Aeronautics and Astronautics Dept., Massachusetts Institute of Technology, Cambridge, MA, 2002.
- [9] Minguet, P., and Dugundji, J., Experiments and Analysis for Composite Blades Under Large Deflections Part I: Static Behavior, AIAA Journal, Vol. 28, No. 9, p. 1573-1579, 1990.
- [10] Chandra, R., Stemple, A. D., and Chopra, I., Thin-Walled Composite Beams Under Bending, Torsional and Extensional Loads, Journal of Aircraft, Vol. 27, No. 7, p. 619-626, 1990.
- [11] Minguet, P., and Dugundji, J., Experiments and Analysis for Composite Blades Under Large Deflections Part II: Dynamic Behavior, AIAA Journal, Vol. 28, No. 9, p. 1580-1588, 1990.
- [12] Cesnik, C. E. S., Cross-Sectional Analysis of Initially Twisted and Curved Composite Beams, Ph.D. Dissertation, School of Aerospace Engineering, Georgia Institute of Technology, Atlanta, GA, 1994.
- [13] Hodges, D. H., Atilgan, A. R., Fulton, M. V., Rehfield L. W., Free Vibration Analysis of Composite Beams , American Helicopter Society National Specialists Meeting on Rotorcraft Dynamics, Arlington, Texas, 1989.
- [14] Chandra, R., and Chopra, I., Experimental-Theoretical Investigation of the Vibration Characteristics of Rotating Composite Box Beams, Journal of Aircraft, Vol. 29, No. 4, p. 657-664, 1992.

## 8. COPYRIGHT STATEMENT

The authors confirm that they, and/or their company or organization, hold copyright on all of the original material included in this paper. The authors also confirm that they have obtained permission, from the copyright holder of any third party material included in this paper, to publish it as part of their paper. The authors confirm that they give permission, or have obtained permission from the copyright holder of this paper, for the publication and distribution of this paper as part of the ERF2013 proceedings or as individual offprints from the proceedings and for inclusion in a freely accessible web-based repository.

## 9. APPENDIX

### 9.1. Figures

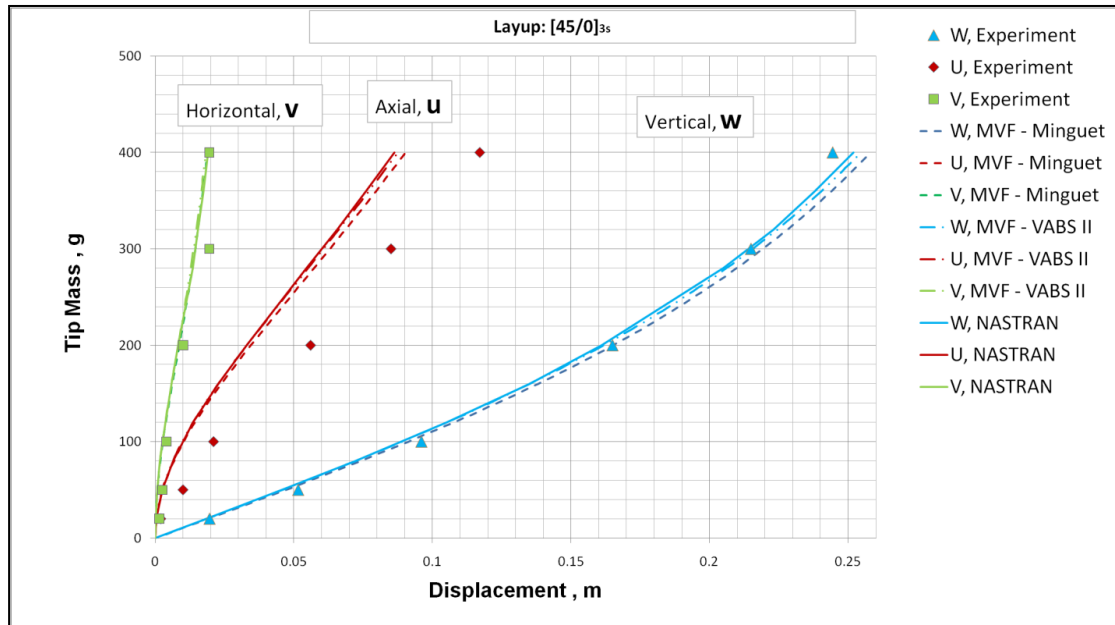


Figure 2. Static deflection results for [45/0]<sub>3s</sub> layup.

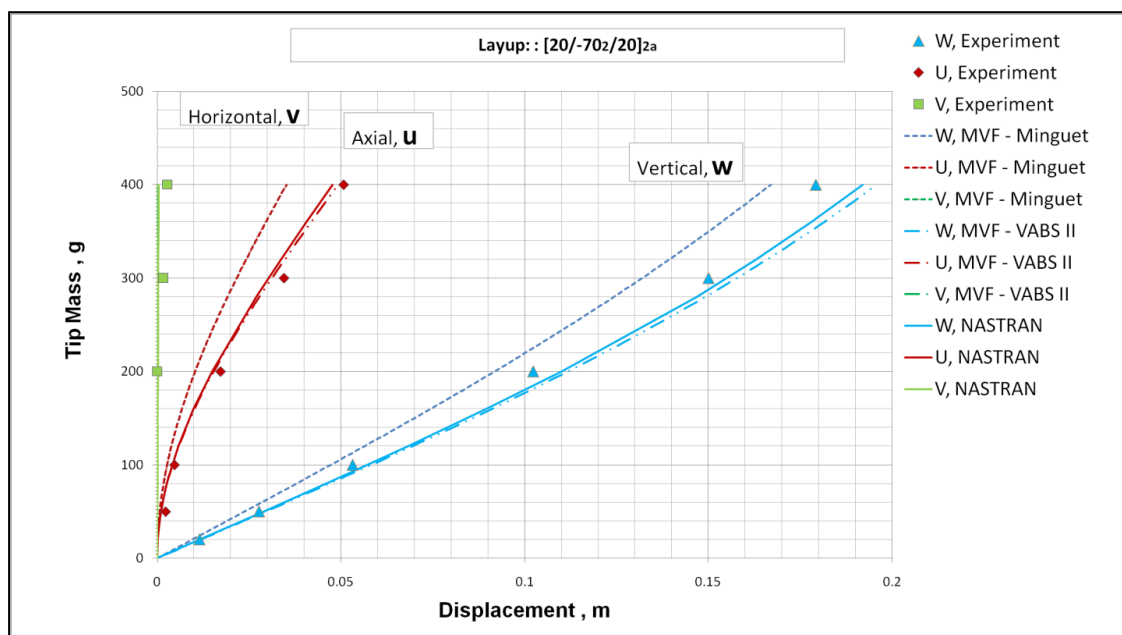


Figure 3. Static deflection results for [20/-70/-70/20]<sub>2a</sub> layup.

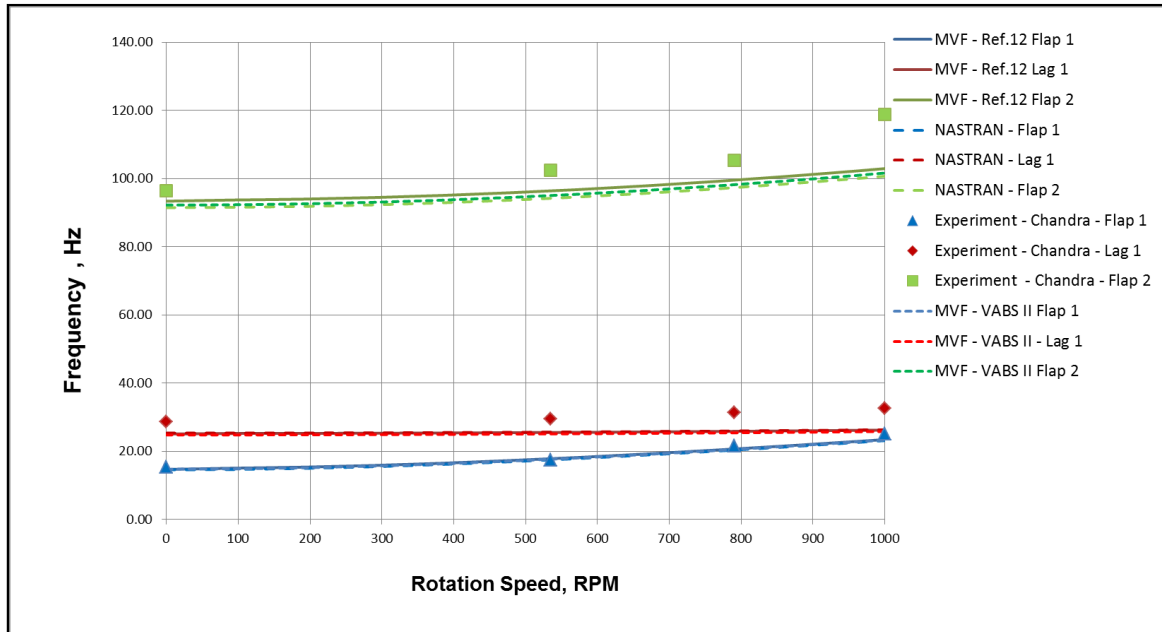


Figure 4. Rotating natural frequencies of  $[45]_6$  graphite-epoxy box beam

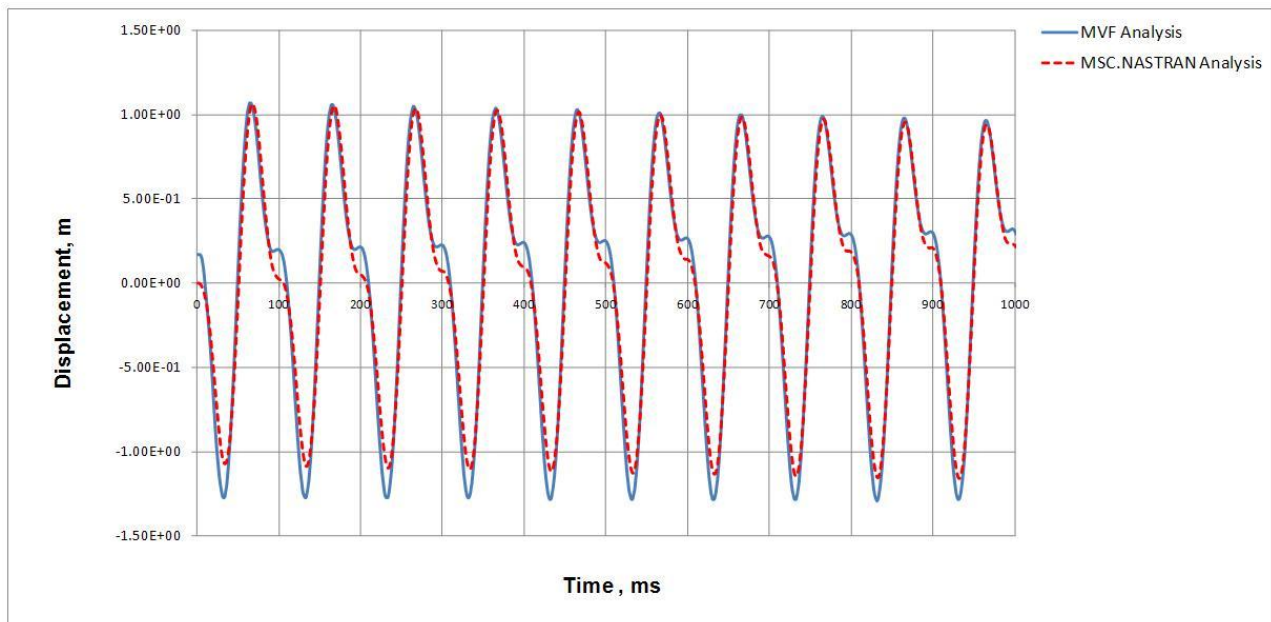


Figure 5. Response for 10 Hz harmonic forcing at the tip for 80 rad/s rotation speed

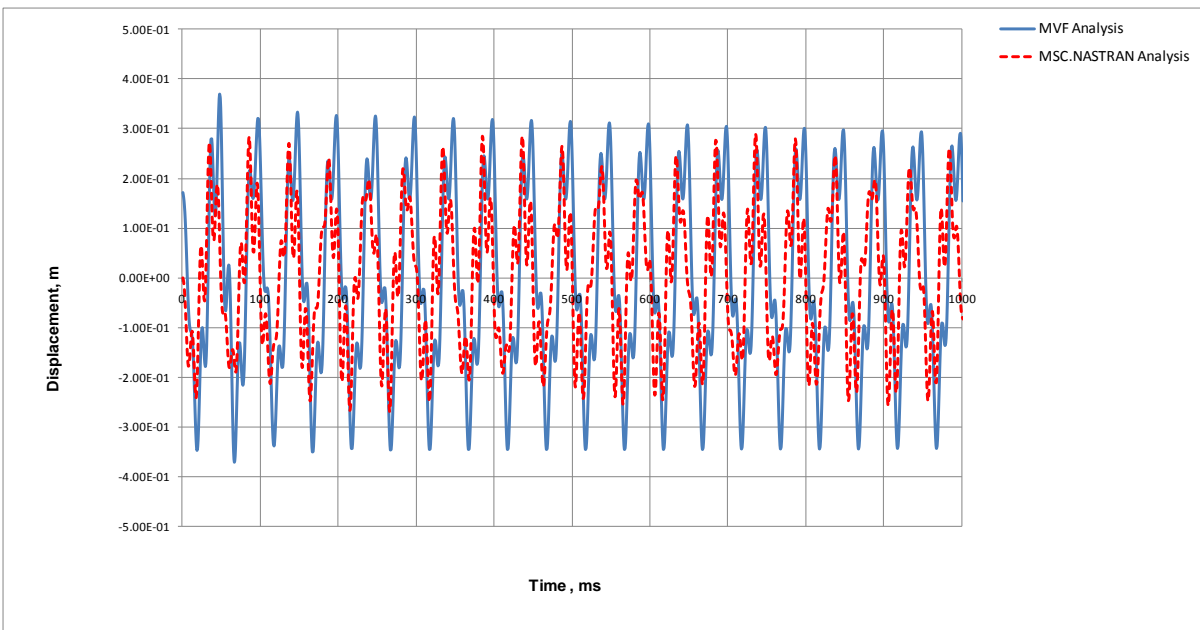


Figure 6. Response for 80 Hz harmonic forcing at the tip for 80 rad/s rotation speed

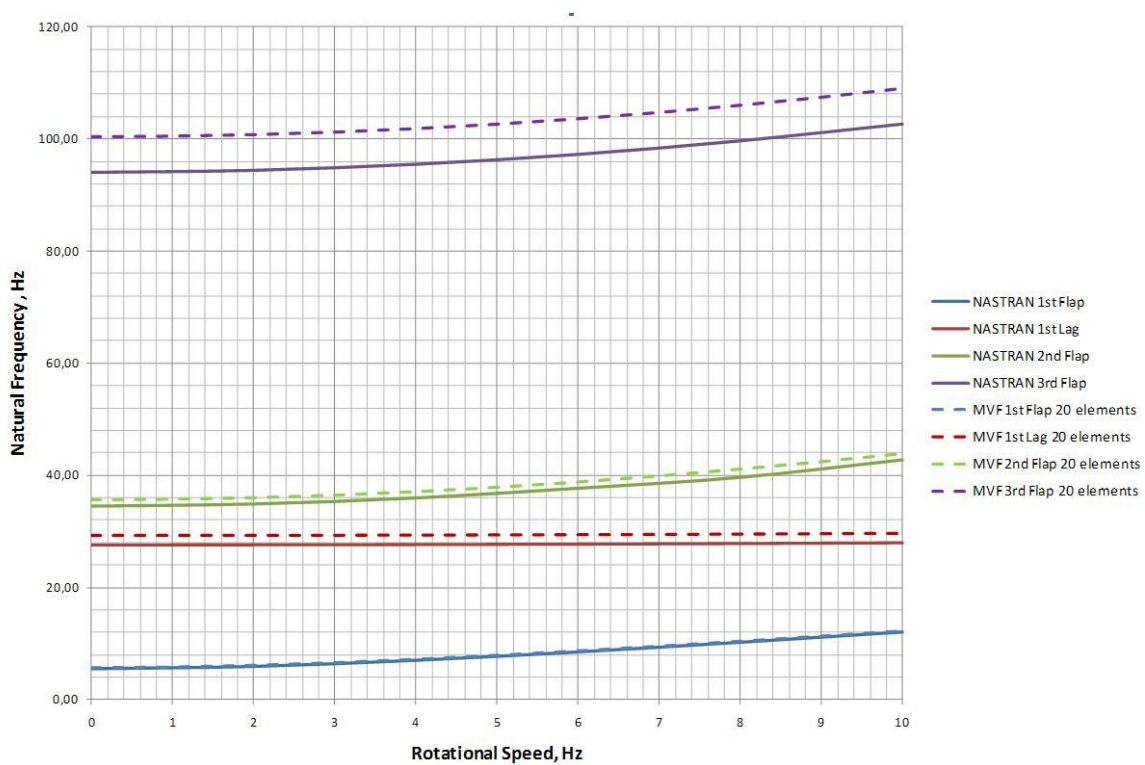


Figure 7. Rotating natural frequencies for hypothetical blade

## 9.2. Tables

**Table 1. Sectional Analysis Results for [0/90]<sub>3s</sub> layup**

Stiffness Results (N,Nm,Nm<sup>2</sup>) 1 Extention; 2,3 Shear; 4 Torsion; 5,6 Bending

	MINGUET [REF.9]	VABS II Analysis - (12x100 Elm.)
S11	3.70E+06	3.35E+06
S22	2.60E+05	2.21E+05
S33	2.90E+05	2.02E+05
S44	1.83E-01	1.84E-01
S55	7.07E-01	7.33E-01
S66	2.76E+02	2.51E+02

**Table 2. Sectional Analysis Results for [45/0]<sub>3s</sub> layup**

Stiffness Results (N,Nm,Nm<sup>2</sup>) 1 Extention; 2,3 Shear; 4 Torsion; 5,6 Bending

	NABSA [REF.12]	VABS [REF.12]	MINGUET [REF.9]	VABS II Analysis - (12x100 Elm.)
S11	3.61E+06	3.61E+06	4.00E+06	3.62E+06
S12	-2.07E+05	-2.08E+05	2.70E+05	2.06E+05
S22	4.17E+05	4.19E+05	2.60E+05	4.16E+05
S33	3.06E+04	2.11E+05	5.50E+05	3.10E+04
S44	3.59E-01	3.70E-01	3.68E-01	3.61E-01
S45	9.92E-02	1.05E-01	1.02E-01	9.98E-02
S55	5.31E-01	5.35E-01	5.22E-01	5.35E-01
S66	2.63E+02	2.63E+02	2.98E+02	2.64E+02

**Table 3. Sectional Analysis Results for [20/-70/-70/20]<sub>2a</sub> layup**

Stiffness Results (N,Nm,Nm<sup>2</sup>) 1 Extention; 2,3 Shear; 4 Torsion; 5,6 Bending

	NABSA [REF.12]	VABS [REF.12]	MINGUET [REF.9]	VABS II Analysis (16x100)
S11	3.37E+06	3.38E+06	3.90E+06	3.37E+06
S14	-9.70E+02	-9.72E+02	5.22E+02	-9.60E+02
S22	5.89E+05	7.65E+05	1.10E+06	5.90E+05
S25	4.11E+02	4.38E+02	-	4.11E+02
S33	4.42E+04	2.57E+05	1.20E+05	4.76E+03
S36	7.01E+00	2.29E-05	-	7.08E-01
S44	1.05E+00	1.64E+00	1.18E+00	1.05E+00
S55	1.08E+00	1.05E+00	9.83E-01	1.08E+00
S66	2.43E+02	2.44E+02	2.90E+02	2.43E+02

**Table 4. Free Vibration Results, frequencies, hz**

Layup	Method	Flap Bending Modes (hz)			Torsion (hz)	Lag (hz)
		Mode #1	Mode #2	Mode #3	Mode #1	Mode #1
[0/90]3s	Minguet-Experimental	5.70	34.00	98.00	62.00	-
	Minguet-Analytical (NL)	5.70	36.00	101.00	68.00	126.0
	Blevins-Analytical*	5.74	35.98	100.74	-	-
	MVF - 20 elm*(minguet)	5.75	36.46	104.39	84.46	112.6
	MVF - 20 elm*(VABS II)	5.85	37.12	106.28	84.69	107.3
	MVF - 20 elm**(VABS II)	5.76	36.51	104.53	83.32	105.6
	MVF - 20 elm*** (VABS II)	5.54	35.15	100.62	80.17	101.6
	NASTRAN3D**	5.88	36.87	103.24	87.65	106.4
	NASTRAN3D***	5.66	35.49	99.39	84.27	102.5
	NASTRAN3D**(NL)	5.89	36.87	103.23	82.50	110.0
	NASTRAN3D*** (NL)	5.67	35.49	99.37	78.75	106.4
[45/0]3s	Minguet-Experimental	4.30	28.00	78.00	135.00	-
	MVF - 20 elm**(minguet)	4.75	30.15	86.30	118.56	115.7
	MVF - 20 elm*** (minguet)	4.55	28.84	82.54	113.38	110.7
	MVF - 20 elm**(VABS II)	4.82	30.54	87.32	117.45	109.4
	MVF - 20 elm*** (VABS II)	4.61	29.21	83.51	112.29	104.6
	NASTRAN3D**	4.83	30.24	84.69	119.74	109.2
	NASTRAN3D***	4.62	28.92	80.98	114.50	104.5
	NASTRAN3D**NL	4.84	30.25	84.67	133.13	94.9
	NASTRAN3D***NL	4.63	28.92	80.96	128.72	89.2
[20/-70/-70/20]2a	Minguet-Experimental	5.80	36.00	103.00	166.00	-
	MVF - 20 elm**(minguet)	5.87	37.23	106.56	180.14	100.6
	MVF - 20 elm*** (minguet)	5.56	35.24	100.85	170.48	95.2
	MVF - 20 elm**(VABS II)	5.27	33.18	93.88	150.60	92.0
	MVF - 20 elm*** (VABS II)	4.99	31.40	88.85	142.52	87.0
	NASTRAN3D**	5.31	33.29	93.27	152.49	92.5
	NASTRAN3D***	5.03	31.50	88.27	144.32	87.5
	NASTRAN3D**NL	5.32	33.29	93.24	155.72	89.6
	NASTRAN3D***NL	5.03	31.51	88.24	148.07	84.2

\* ρ calculated from beam mass distribution

\*\*ρ according to ply properties

\*\*\*ρ normalized according to laminate thickness